17th World Conference on Earthquake Engineering, 17WCEE
Sendai, Japan - September 13th to 18th 2020

3D FE ANALYSIS OF A BASE-ISOLATED BUILDING CONSIDERING STRUCTURAL COLLISIONS WITH MOAT WALLS

D. Kim[(1)], Y. Miyamoto [(2)]

[(1)] *Civil Engineer, Daiwa House Industry Co., Ltd, Osaka, Japan, kdhendrix90@gmail.com*
[(2)] *Professor, Department of Global Architecture, Osaka University, Osaka, Japan, miyamoto@arch.eng.osaka-u.ac.jp*

Abstract

Base isolation is a widely accepted method to introduce high-level seismic safety to structures around earthquake-prone zones in the world. The key concept of base isolation is to separate a superstructure from the ground by implementing isolation devices allowing the superstructure to move sideways to mitigate structural damage during seismic events. In order to compensate the sideways motion, moat walls are constructed to introduce a gap distance between the superstructure and surrounding soil. A gap distance is designed to be under the maximum-predicted lateral displacement of the isolation devices to avoid structural collisions with the moat walls. However, during extreme seismic events with catastrophic magnitude or predominant long-period components, the lateral displacement may exceed the gap distance and the building base collides with the moat walls. This phenomenon is referred to as the earthquake-induced structural collision with moat walls. In spite of the recent growing concerns on the probability in occurrence of structural collisions in base isolation, only a handful of large-scale experiments or finite element analyses were conducted due to the complexity of the phenomenon. In this paper, a series of nonlinear dynamic finite element analyses were conducted to investigate the seismic behavior of a base-isolated structure considering arbitrary pounding to moat walls. The base-isolated nine-story steel moment-resisting frame, reinforced concrete moat walls, and backfill soil were modeled within a finite dimension in full scale. In order to simulate realistic collisions, a mathematically complex concrete material model was applied with explicitly embedded reinforcing bars for the moat walls. Four different bidirectional ground motions were applied to induce various types of arbitrary poundings. From these analyses, the following results were obtained: a) The superstructure experienced large floor accelerations, story drifts, torsional, and rocking responses especially on lower floors during poundings. b) Base isolators showed a dramatic change in vertical force due to temporary compressive and tensile forces generated during poundings. c) Pounding to moat walls can easily induce localized damage or even excessive failure of not only the superstructure but also the moat walls and backfill soil. d) The response patterns of the simulation model varied depending on the seismic characteristics of the input ground motions.

Keywords: Base Isolation; Moat Walls; Structural Collision; Full-Scale Nonlinear FE Analysis

1. Introduction

Base isolation has been widely implemented to a large amount of buildings worldwide to mitigate seismic damage to buildings since the advent of the technology. The key concept of base isolation is to decouple the base of a building from the ground by introducing isolation devices whose hysteretic behaviors absorb the majority of seismic energy during earthquakes. Instead, the lateral displacement of isolation devices increases largely while dissipating the seismic energy. In order to accommodate the lateral displacement, the and surrounding soil are separated by reinforced-concrete walls referred to as "moat walls" to give enough distance to the base moving sideways freely. The distance between the base and walls is referred to as "gap distance" and it must be under the maximum predicted lateral displacement of isolation devices to prevent pounding to the moat walls during earthquakes. However, the recent seismic probabilistic studies have indicated that the high probability of the occurrence of extreme earthquakes whose seismic intensity may cause isolation devices to deform excessively over their currents gap distances [1, 2].

Pounding between base-fixed structures during earthquakes has been one of the major causes of structural collapses for the past few decades [3, 4]. Therefore, a wide range of both experimental and analytical studies have been conducted to improve the structural safety of base-fixed structures subjected to pounding [5, 6]. Base-isolated buildings colliding with moat walls, by contrast, has not been comprehended thoroughly in the main stream of structural engineering as much as base-fixed buildings, as only few number of pseudo-collision events with non-structural components in the seismic gap were observed [7, 8]. Nevertheless, a handful of advanced experimental and analytical research has been carried out for the last many years to corroborate the current poor understanding on the pounding phenomenon in base isolation.

Miwada et al [9] carried out a real-scale unidirectional pounding experiment with a soon-to-be demolished base-isolated building. Localized structural damage appeared on lower floors and moat walls due to several poundings. Mosqueda et al [10] conducted a series of unidirectional shaking table tests of a down-scale base-isolated structure. The structure suffered from severe floor accelerations and story drifts during poundings, and moat walls showed large plastic deformations. A large number of analytical investigations were also conducted by worldwide researchers such as Komodromos et al [11, 12], Pant et al [13, 14], and Inubushi et al [15]. The studies investigated the response of base-isolated buildings considering pounding to moat walls with commonly used spring-damper contact models. The similar large magnitude of response as shown in the past experimental studies also appeared during the simulations.

However, moat walls were often replaced by rigid planes, and the behavior backfill soil was neglected in many past studies. Multi-directional excitations were not properly considered either, whereas the real pounding events were expected to occur in an arbitrary direction under three dimensional excitations. While base-fixed buildings simply collide with each other, pounding in base isolation is a complex interaction among a building base, isolation devices, moat walls, and backfill soil whose dynamic performances are not structurally clarified under severe impact loads. Therefore, it can be said that the current understanding on pounding in base isolation may not provide proper provisions to ensure the structural safety of base-isolated buildings when pounding occurs.

In this study, large-scale nonlinear dynamic finite element analyses of a base-isolated structure were performed with explicitly modeled reinforced concrete moat walls and backfill soil by the commercial finite element analysis software, LS-DYNA [16]. The main objective of the study was to investigate the response of all relating bodies when the behaviors of moat walls and soil were explicitly considered. An accidental mass eccentricity was also taken into account, where the value was 5 percent of each dimension of the base as suggested in ASCE/SEI 7-10 [17]. Four artificial and recorded near-fault earthquakes were applied bidirectionally to simulate arbitrary in-plane pounding events. In addition, the series of computation works was performed using the semi high-performance computers in Osaka University.

2. Full-scale finite element analyses

2.1 Base-isolated structure modeling

Figure 1 presents the simulation model in detail; the perspective view, section view, and plan view are displayed. The superstructure was a nine-story frame model with 15 columns on each floor. The columns were shear-type beam elements with lumped masses at both ends and floor masses were equally distributed to the 15 floor nodes. Each slab was a set of rigid shell elements on which translational and rotational DOFs were allowed. The base was also rigid but consisted of hexahedral elements. 15 base isolators were placed beneath the base with no geometric eccentricity and the 300mm-thick moat walls surrounded the base with the gap distance of 600mm. The moat walls and base were 3m and 2m-thick in height respectively, thus the base collided with the walls 1m above the bottom plate of the wall. It was referred to as "impact height". The dimension of the soil domain was 60m in width (X) 40m in-depth (Y), and 3.5m (Z) in height and the base was 20m in width, 10m in-depth. The accidental mass eccentricity of the superstructure was 5 percent of each dimension. The superstructure was approximately 28m in height and the total weight was 62,690kN.

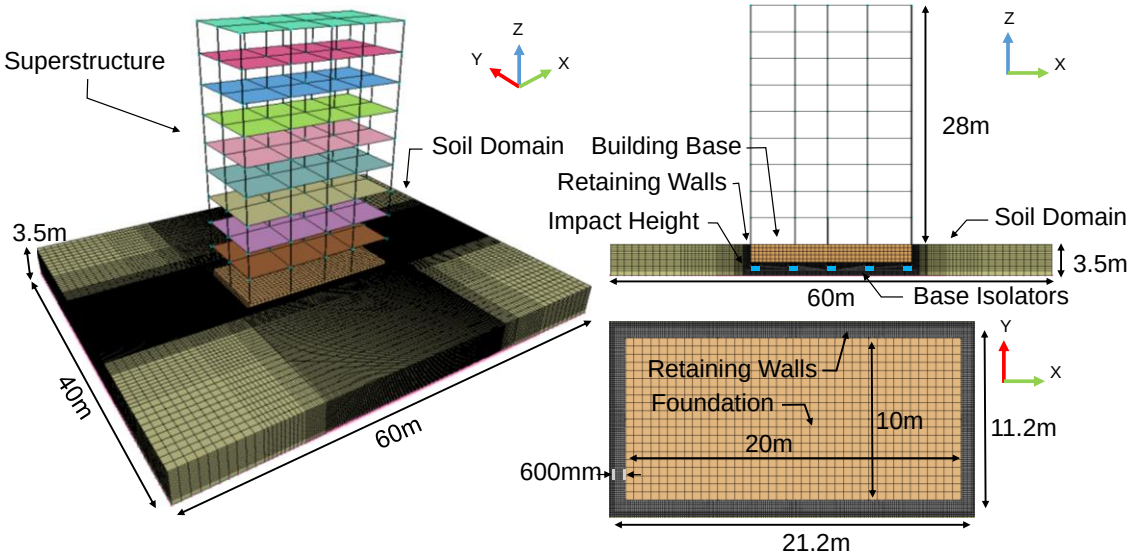

Fig. 1 – Simulation model: perspective view, section view, and plan view

The superstructure consisted of different seismic capabilities on each direction; shear walls were constructed along with the Y direction, thus the fundamental period of the superstructure in the Y direction was 1.5 times shorter than the X direction. This indicates that the structure tended to experience larger structural damage in the X-direction due to its soft lateral stiffness.

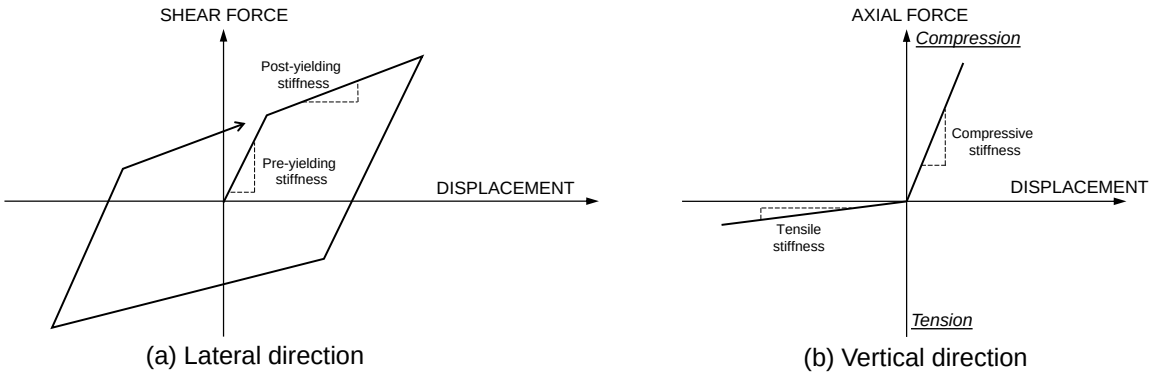

Fig. 2 – Horizontal and vertical characteristics of the base isolator model

Figure 2 presents the horizontal and vertical characteristics of the base isolators. The smooth bilinear hysteresis was adopted for the horizontal behavior, but the vertical behavior of the isolators was described by a linear model with different stiffness values in compression and tension to consider the poor tensile performance of elastomeric isolators. The tensile stiffness was assumed to be one-hundredth of the compressive stiffness. The kinematic hardening of rubber and subsequent failure were not in the scope of this study.

2.2 Reinforced concrete moat walls and backfill soil

The full-scale reinforced concrete moat walls were created as the combination of solid and beam elements that represented concrete and steel bars respectively. Four thin panel-shaped walls facing the four cardinal directions were connected perpendicularly at the bottom plate, which was assumed to behave rigidly (Figure 3).

Figure 4 presents the stress-strain curves for concrete and steel bar elements. Pounding was expected to cause severe plastic deformation of the moat walls, thus complex numerical material models simulating the dynamic performance of reinforced concrete were highly required in this study. The continuous surface cap model, which was developed by the U.S Federal Highway Administration to simulate the dynamic performance of concrete in roadside safety structures, was applied to the concrete elements. Its underlying algorithm simulates not only the linear but also the non-linear failure of concrete under dynamic loads with a strain rate effect [18].

The steel bars were modeled with a standard bi-linear material model considering the strain hardening ratio of 1%. The strain rate effect of the steel bars was also considered due to the significant amount of increase in their yield strength and ultimate strength under dynamic loads. Reinforcement debonding was not considered in this study due to the uncertainty over the dynamic interactions between concrete and reinforcing bars. In addition, in order not to overestimate the plastic deformation capacities of the concrete and reinforcing bars in their post-failure regions, element deletion was applied to cap the plastic strains of both materials.

The backfill soil was modeled by the Mohr-Coulomb failure criterion to simulate the general behavior of sandy soil. The bottom plane of the soil domain was constrained except the translational X and Y directions to input the bidirectional ground motions. The nodes on the lateral boundaries of the soil domain were coupled to move together in the global direction. By coupling each elevation of the outer soil boundaries, the soil domain nearly imitated the free-field condition even with the finite dimension. The penalty-based contact algorithm was applied on the surface of solid elements to consider three-dimensional contacting among the base, moat walls, and soil domain. The algorithm detects penetration on the surface due to contact and calculated a force proportional to the indentation depth to offset the penetration.

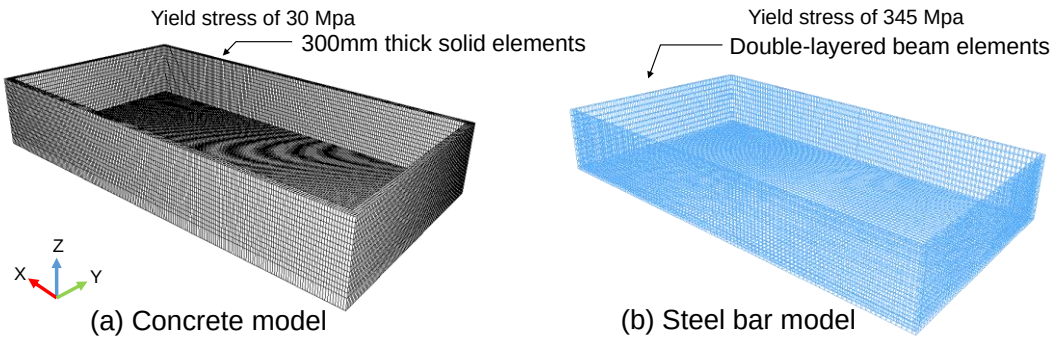

Fig. 3 – Reinforced concrete moat walls

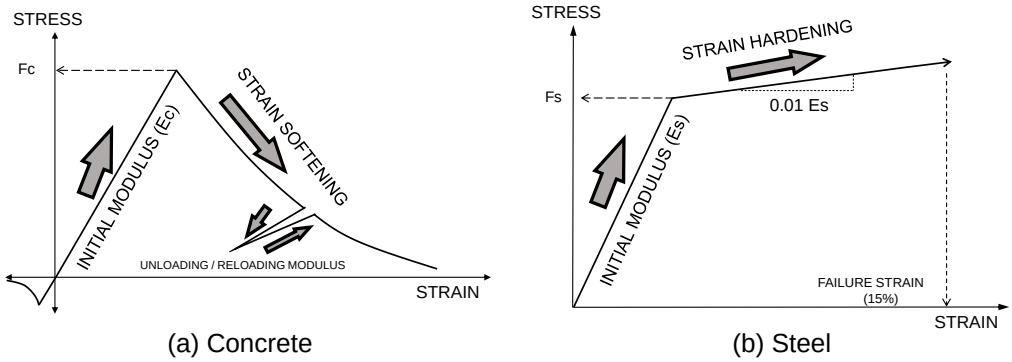

Fig. 4 – Single element stress-strain results for (a) concrete and (b) steel bar

2.3 Input ground motions

Four sets of bidirectional artificial and recorded ground motions were applied to the simulation model. Each one of the sets induces the lateral displacement of the base isolators over the given gap distance (Table 1 and Figure 5). All earthquake accelerograms were retrieved from web-based public earthquake databases and a seismic probabilistic study [18].

Table 1 Seismic properties of input ground motions

Case Name	Event Name (Region - Type)	Mw	Station Code	Direction	PGA [cm/s^2]	PGV [cm/s]	Scale Factor
GM 1	Uemachi Fault Earthquake (Japan - Artificial)	7.0	A4-3C-1-Flat	EW (Y) NS (X)	1048 705	104 80.1	1.0
GM 2	2016 Kumamoto Earthquake (Japan - Recorded)	7.1	KMM004	EW (Y) NS (X)	352 264	75.5 65.8	1.0
GM 3	2010 Darfield Earthquake (New Zealand - Recorded)	7.1	CHHS	EW (Y) NS (X)	177 246	31.2 93.4	1.2
GM 4	1999 Chi-Chi Earthquake (Taiwan - Recorded)	7.6	TCU068	EW (Y) NS (X)	499 362	32.2 34.7	1.0

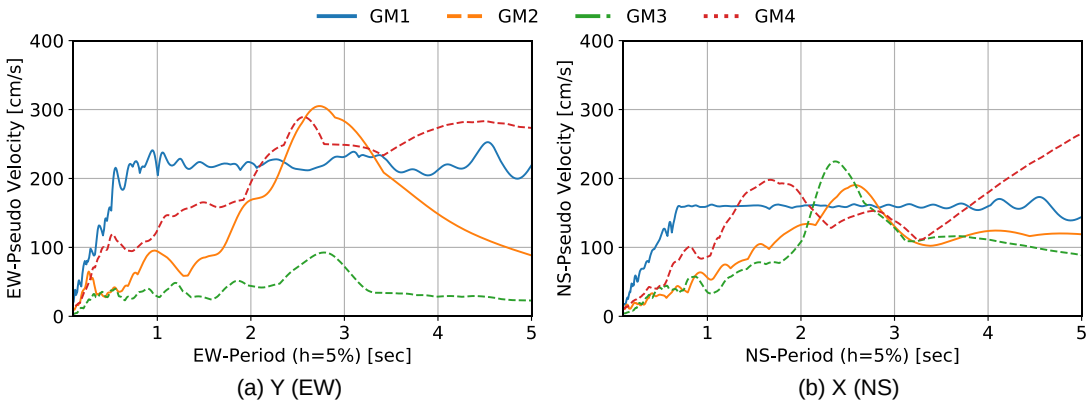

Fig. 5 – Pseudo velocity response spectra of each ground motion

3. Analysis results

The effect of pounding on the response of the base-isolated structure model was analyzed here with a wide range of viewpoints to earn detailed explanations on the pounding phenomenon. Not only the superstructure per se, but also the base isolators, moat walls, and backfill soil showed unrealistically large response during

the simulations. Furthermore, the four different ground motion sets gave rise to diverse pounding excursions of the base which led to various yielding and failure patterns of the moat walls and nearby soil.

3.1 Response of moat walls and backfill soil

Figure 6 presents the bidirectional behavior of the four isolators located near the four corners during each analysis. The red dashed lines represent the 600mm gap distance to the moat walls. Each case showed multiple arbitrary poundings to the moat walls, except the analysis of GM3 which showed a single pounding to the north wall almost perpendicularly. Even after the base contacted the moat walls, it kept moving forward and the lateral displacement of the corner isolators reached approximately 450% when GM1, GM2, and GM4 were applied. The known maximum lateral displacement capacity of an elastomeric isolator is usually under 400%. The results clearly indicate that the base isolators may deform over their ultimate deformation capacities, even if the moat walls and backfill soil blocked the base from moving further to a certain extent during pounding events. Furthermore, it is worth noting that the corner isolators deformed laterally by 30% more than the central isolators due to the in-plane torsion of the base. This strongly implies that the displacement demand for the corners isolators needs to be evaluated carefully when considering the mass eccentricity.

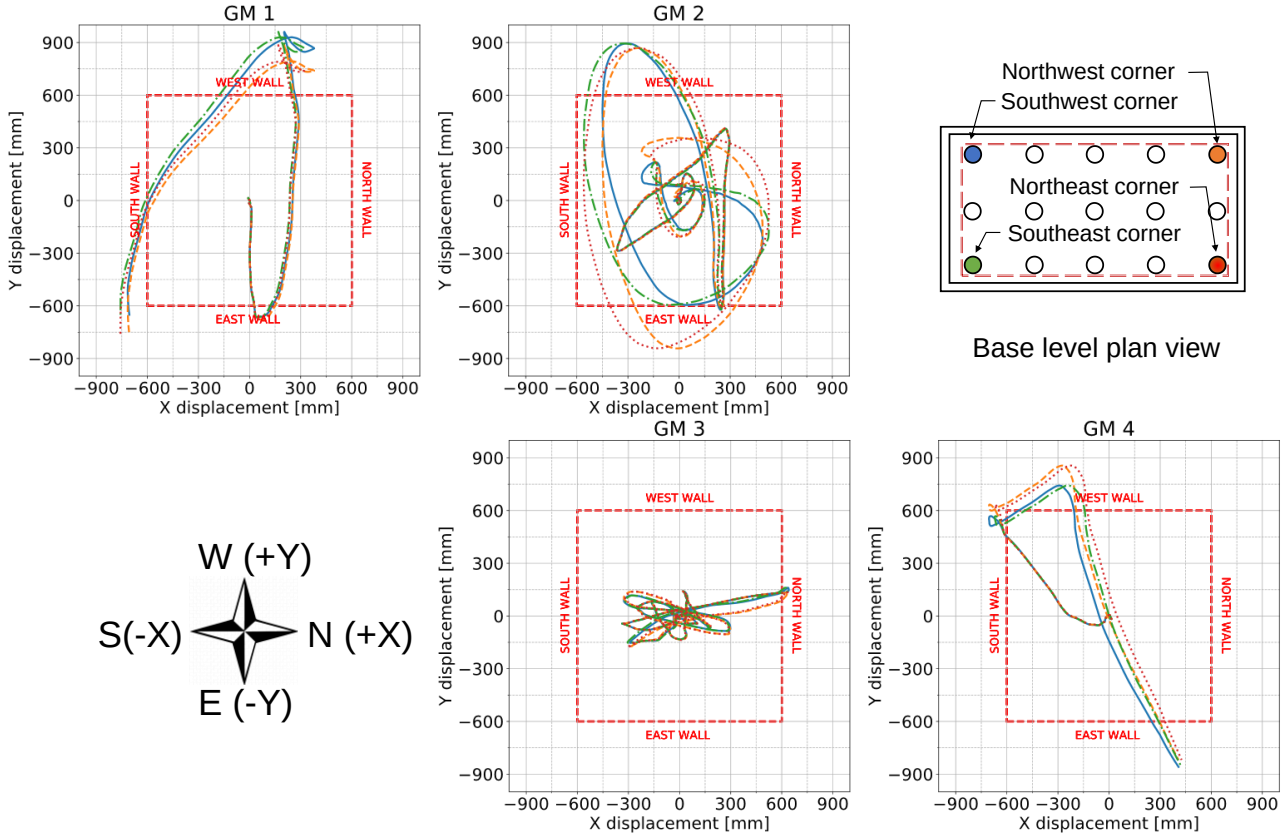

Fig. 6 – Bidirectional behavior of isolators located on the four corners by the four ground motions

Figure 7 presents the effective plastic strain distribution on the moat walls and backfill soil at the end of each analysis. The widespread plastic deformations were seen on both bodies due to the multiple poundings. It should be noted that the reinforced concrete elements were not capable of enduring stress anymore once they failed in order to cap the maximum deformation of the elements. When GM3 was applied, for instance, hardly any soil elements around the north wall showed plastic deformation after pounding, as the wall was stiff enough to dissipate the impact energy by itself. On the other hand, the other three cases displayed large plastic deformations of the backfill soil. This was caused by the structural damage on the corners of the walls during pounding. The analysis of GM1 showed three poundings to the west, east and north walls in order. During the first two impacts, SW and SE corners underwent severe damage leading to the high plastic strain on the south

wall. As a result of this, the backfill soil had a large plastic deformation, as the seismic capacity of the south wall had already been significantly reduced. After the four corners yielded or even failed, the moat walls were no longer capable of preventing the base from moving further. In this stage, the wall behaved partially like a cantilever beam undergoing bending deformation at the bottom, and shear deformation around the impact height.

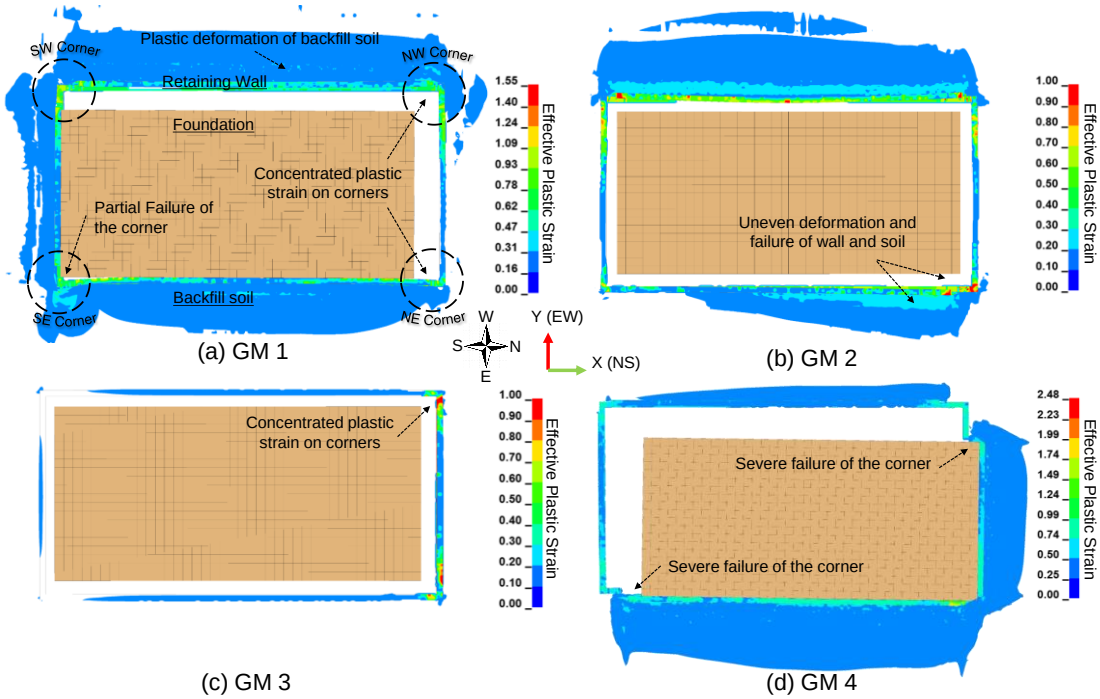

Fig. 7 – Effective plastic strain distribution on moat walls and backfill soil at the end of each analysis

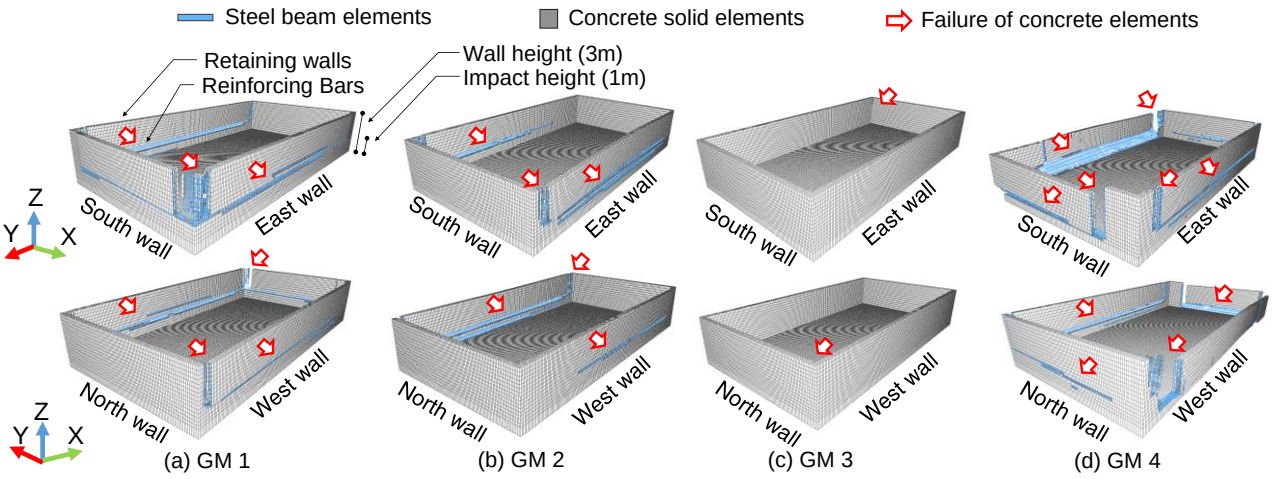

Fig. 8 – Failure of concrete and reinforcing bar elements of moat walls at the end of each analysis

Figure 8 presents the failure of concrete and steel bar elements of the moat walls at the end of each analysis. The embedded bars were partly exposed in the air due to the multiple poundings, as the element erosion was applied to the concrete and steel bars, limiting their maximum plastic strains. The failure patterns may differ from that of another; however, the results clearly imply that the four corners and the wall elements around the impact height played important roles in sustaining the impact loadings. The walls behaved as a

cantilever beam with a concentrated load at the impact height at the beginning of pounding. At this initial stage, the wall was governed by bending deformation with a plastic hinge line formed at the bottom of the wall, but thereafter another plastic hinge was formed at the impact height over the course of time. However, this second hinge disappeared shortly afterward due to the subsequent shear failure of concrete elements, which resulted in the U-shaped deformation patterns on the walls. Therefore, it is obvious that the moat walls were not an isotropic body but rather had concentrated stiffness at the four corners, and plastic deformations of the wall elements around the impact height governed the failure patterns of the moat walls.

3.2 Response of the superstructure and base isolators

Not only the moat walls and backfill soil, but also the superstructure and base isolators were subject to structural damage when pounding occurred. Figure 9 presents the maximum floor accelerations and story drifts of the superstructure at the central columns. It is obvious that the superstructure showed absolutely different response patterns during the analyses in both directions due to the difference in the lateral stiffness.

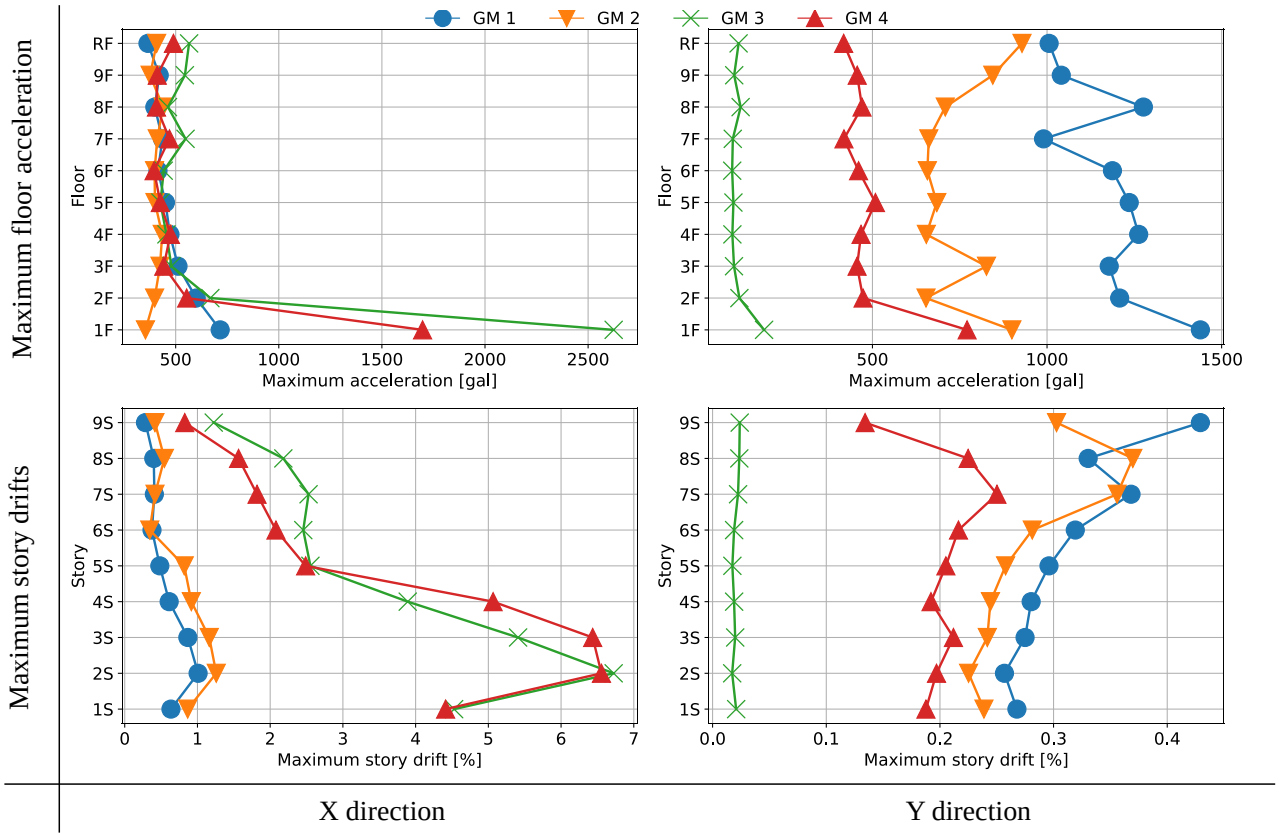

Fig. 9 – Maximum floor acceleration and Maximum story drifts of the superstructure in X and Y directions

The superstructure in X direction whose lateral stiffness was approximately 9 times smaller than Y direction underwent severe floor accelerations and story drifts at the same time, but they were mostly concentrated on the lower floors. The maximum values of over 1500gal floor acceleration were observed on the first floor and the story drifts also sored to nearly 7% under GM 3 and GM 4. Hardly any structural pounding occurred in X direction under GM 1 and GM 2 compare to the ones in Y direction or the impact velocity was too small even pounding occurred. On the other hand, relatively even response patterns were observed on every floor in Y direction whose lateral stiffness seemed large enough to endure the impact loads. The maximum value of 1000gal to 1500gal floor accelerations were observed, but the story drifts only increased to the maximum value of 0.4% evenly on every floor. It showed that the superstructure in Y direction maintained the structural integrity even under severe impact loads, but instead every floor suffered from the

large floor accelerations. The high acceleration pulses due to poundings, nevertheless, only lasted during one-hundredth seconds. Furthermore, it is worth noting that the yielding of base-isolated structures is strongly inadvisable due to the unwanted secondary damage by resonance. In general, stiffness degradation helps base-fixed structures avoid earthquake-induced resonance which amplifies structural damage. On the contrary, as the fundamental period of a base-isolated structure is determined by the lateral stiffness of base isolators, the nonlinear behavior of a superstructure barely changes the fundamental period. As a result of this, a superstructure whose natural periods have been enlengthened due to nonlinear deformations resonates with the long-period waves filtered by the isolated base. This is the reason that the superstructure in X direction underwent more structural damage due to nonlinear deformation and its subsequent resonance effect.

One may suggest that the yielding of the superstructure may stop the base from proceeding further due to the redistribution of seismic energy between the superstructure and isolators. However, the simulation results clearly indicate that the low lateral stiffness may reduce the floor accelerations, but nonetheless, it undeniably jeopardizes the entire structural integrity. Increasing the lateral stiffness to endure high impact forces, on the other hand, may prevent structural collapse, whereas the pulse accelerations can still be disastrous for structures with high-level resilience plans such as hospitals, data centers, and airports.

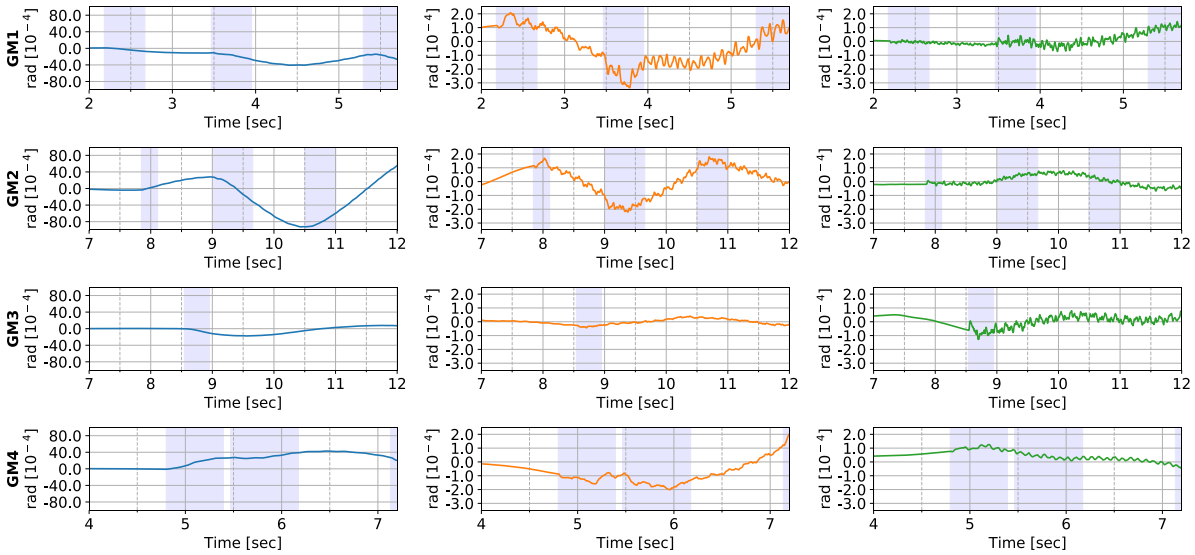

Fig. 10 – Torsional and rotational response of the base

Figure 10 presents the torsional and rocking response time histories of the base. The blue spans describe the duration of each pounding. The simulation model showed complicated three-dimensional translational and rotational behaviors not only by the seismic excitations, but also by the multiple arbitrary poundings. It was found that the mass eccentricity of 5% in both directions caused the in-plane torsion and its degree was slightly amplified during the poundings (Figure 10-(a)). Moreover, the torsion of the base caused unequal distribution of the impact force leading to the subsequent uneven yielding or failure of the walls. As a consequence, the corner isolators tended to sustain the larger deformation than the central isolators, as shown in Figure 6.

The rocking response of the structure was also well-observed from the results (Figure 10-(b), (c)). Most cases showed larger rocking response around the Y-direction, as the majority of the pounding events were to the east/west walls. Long-lasting high-frequency waves appeared indicating the structure underwent severe dynamic rocking motions, especially after poundings.

4. Conclusion

This study conducted a series of full-scale nonlinear dynamic finite element analyses to investigate the seismic response of a base-isolated structure considering multiple arbitrary pounding to moat walls under extreme

ground motions. A detailed investigation of the influence of structural pounding discovered that pounding in base isolation largely jeopardized the structural integrity of the base-isolated structure. Not only did the superstructure and base isolators undergo the large floor accelerations, story drifts, in-plane torsion, and rotational motions but also the moat walls, and backfill soil showed severe plastic deformation or failure to a certain extent. The conclusions obtained from this study are as follows:

- The surrounding backfill soil plays a pivotal role in dissipating impact energy during pounding. The degree of the stain, however, was highly related to the deformation of the wall. Accordingly, the backfill soil must be taken into account to corroborate the current shortcomings of pounding simulations. Furthermore, it should be noted that the area of the deformed soil was greatly dependent on the impact velocity, impact angle, and contact time of each pounding.
- The moat walls show a three-dimensional distribution of stiffness causing uneven yielding and failure. Two plastic hinge lines were formed at the bottom and around the impact height due to pounding. The moat wall behaved as a cantilever beam within the elastic range forming a plastic hinge at the bottom of the wall. However, with the base pushing the wall forward, another plastic hinge appeared around the impact height due to the severe shear failure of concrete elements around the height. More importantly, the corners of the moat walls have a higher value of stiffness than other areas, as they are firmly constrained by two walls crossing orthogonally. Therefore, the modeling of the reinforced concrete moat walls must account for the location-dependent stiffness and subsequent deformation capacity thoroughly for advanced pounding analysis.
- Structural pounding amplifies strong in-plane torsion and rocking motions to the entire base isolation system. The response of the superstructure can be explained as a lever using the wall as a fulcrum. The lower floors are almost immediately decelerated, but the upper floors keep moving forward due to the inertia of motion during pounding. As a result of this, the base isolators underwent considerable rocking motions causing dynamic high-frequency downward and upward forces leading to the instable behavior of the isolators.
- The lateral stiffness of the superstructure highly affects the response of the superstructure during pounding. Two different impact response patterns were observed from the results. The superstructure in the X-direction displayed extremely large floor accelerations and story drifts on lower floors than the upper floors. It implies that the lower floors were not stiff enough to endure the impact force so that they deformed exceedingly. On the other hand, The Y-direction showed large pulse accelerations but insignificant story drifts on every floor but relatively uniform response pattern along with the height due to its high lateral stiffness.

This study provided a wide range of results to gain a broader understanding and appreciation of the structural pounding in base isolation, despite the limited amount of cases due to high computation loads. Therefore, the influence of pounding on the response of base-isolated structures with more analytical cases and experimental verifications remains to be further investigated.

5. References

[1] Earthquake Research Committee (2018): National Seismic Hazard Maps for Japan 2018. *The headquarters for earthquakes research promotion*, Tokyo, Japan (In Japanese).

[2] Cascadia Region Earthquake Workgroup (2013): Cascadia Subduction Zone Earthquakes. A Magnitude 9.0 Earthquake Scenario, Oregon, USA.

[3] Rosenblueth E, Meli R (1986): The 1985 Earthquake: Causes and Effects in Mexico City. *Concrete International*, 8, 23-24.

[4] Cole GL, Dhakal R, Chouw N (2012): Building Pounding Damage Observed in the 2011 Christchurch earthquake Christchurch Earthquake. *15th World Conference on Earthquake Engineering*, Lisbon, Portugal.

[5] Jankowski R, Mahmoud S (2016). *Earthquake-Induced Structural Pounding*. Springer International Publishing.

[6] Merriman P, Williams MS, Blakeborough A (2019): The Northridge, California earthquake of 17 January 1994. *Institution of Structural Engineer*, Los Angeles, USA.

[7] Nagarajaiah S, Sun X (2001): Base-Isolated FCC Building: Impact Response in Northridge Earthquake. *Journal of Structural Engineering, 127(9)*. https://doi.org/10.1061/(ASCE)0733-9445(2001)127:9(1063).

[8] Gavin H, Wilkinson G (2010): Preliminary observations of the effects of the 2010 Darfield earthquake on the base-isolated Christchurch Women's Hospital. *Bulletin of the New Zealand Society for Earthquake Engineering, 43(4):360-367*. https://doi.org/10.5459/bnzsee.43.4.360-367.

[9] Miwada G, Komaki J, Sato K, Sano T, Katsumata H, Takiyama N, Hayashi Y (2011): Experiments and Simulation Analysis of Collision to Retaining Wall with Real Scale Base-Isolated Building. *Journal of Structural and Construction Engineering, 76(663), 899-908.* https://doi.org/10.3130/aijs.76.899 (In Japanese).

[10] Masroor A, Mosqueda G (2013): Seismic Response of Base-Isolated Buildings Considering Pounding to Moat Walls. *Multidisciplinary Center for Earthquake Engineering Research (MCEER), 13-0003*. Berkeley, USA.

[11] Polycarpou PC, Komodromos P (2010): Simulating seismically isolated buildings under earthquake-induced pounding incidences. *Structures Under Shock and Impact XI, 113:245*. https://doi.org/10.2495/SU100211.

[12] Mavronicola EA., Polycarpou PC, Komodromos P (2017): Spatial Seismic Modeling of Base-Isolated Buildings Pounding against Moat Walls: Effects of Ground Motion Directionality and Mass Eccentricity. *Earthquake Engineering & Structural Dynamics, 46(7): 1161–79*. https://doi.org/10.1002/eqe.2850

[13] Pant DR., Wijeyewickrema AC (2012): Structural Performance of a Base-Isolated Reinforced Concrete Building Subjected to Seismic Pounding. *Earthquake Engineering & Structural Dynamics, 12, 1709–16.* https://doi.org/10.1002/eqe.2158.

[14] Pant DR, Wijeyewickrema AC (2019): Nonlinear seismic response of base-isolated buildings considering pounding. *8th International Conference on Urban Earthquake Engineering*, Tokyo, Japan.

[15] Inubushi T, Miyamoto Y, Yamashita T, Enomoto T (2015): Study on simple modeling for lateral resistance of retaining wall in collision with a base-isolated structure. *Journal of Structural and Construction Engineering (Transactions of AIJ), 80. 1033-1043*. https://doi.org/10.3130/aijs.80.1033.

[16] LS-DYNA (2018): Multi-physical finite element program. Livermore Software Technology Corporation. Livermore, USA.

[17] American Society of Civil Engineers (2010). Minimum design loads for buildings and other structures, *ASCE/SEI 7-10*, Reston, USA.

[18] Murray YD (2007); User's manual for LS-DYNA concrete material model 159. *US Department of Transportation Federal Highway Administration, FHWA-HRT-05-062*.

